

# Crystal growth in aqueous hydrofluoric acid and $(\text{HF})_x \cdot \text{pyridine}$ solutions: syntheses and crystal structures of $[\text{Ni}(\text{H}_2\text{O})_6]^{2+} [\text{MF}_6]^{2-}$ ( $\text{M} = \text{Ti}, \text{Zr}, \text{Hf}$ ) and $\text{Ni}_3(\text{py})_{12}\text{F}_6 \cdot 7\text{H}_2\text{O}$ $\star$

Paramasivan Halasyamani, Michael J. Willis, Charlotte L. Stern, Kenneth R. Poeppelmeier  $\star$

*Department of Chemistry, Northwestern University, Evanston, IL 60208, USA*

Received 30 December 1994; revised 13 March 1995

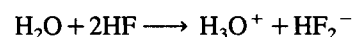
## Abstract

The syntheses and structures of  $[\text{Ni}(\text{H}_2\text{O})_6]^{2+} [\text{MF}_6]^{2-}$  ( $\text{M} = \text{Ti}, \text{Zr}, \text{Hf}$ ) and  $\text{Ni}_3(\text{py})_{12}\text{F}_6 \cdot 7\text{H}_2\text{O}$  are reported. The former three compounds are isostructural, crystallizing in the trigonal space group  $R\bar{3}$  (No. 148) with  $Z=3$ . The lattice parameters are  $a=9.489(4)$ ,  $c=9.764(7)$  Å, with  $V=761(1)$  Å<sup>3</sup> for Ti;  $a=9.727(2)$ ,  $c=10.051(3)$  Å, with  $V=823.6(6)$  Å<sup>3</sup> for Zr; and  $a=9.724(3)$ ,  $c=10.028(4)$  Å, with  $V=821.2(8)$  Å<sup>3</sup> for Hf. The structures consist of discrete  $[\text{Ni}(\text{H}_2\text{O})_6]^{2+}$  and  $[\text{MF}_6]^{2-}$  octahedra joined by  $\text{O}-\text{H}\cdots\text{F}$  hydrogen bonds. Large single crystals were grown in an aqueous hydrofluoric acid solution.  $\text{Ni}_3(\text{py})_{12}\text{F}_6 \cdot 7\text{H}_2\text{O}$  crystallizes in the monoclinic space group  $I2/a$  (No. 15) with  $Z=4$ . The lattice parameters are  $a=16.117(4)$ ,  $b=8.529(3)$ ,  $c=46.220(7)$  Å,  $\beta=92.46(2)^\circ$ , and  $V=6348(5)$  Å<sup>3</sup>. The structure consists of discrete  $\text{Ni}(\text{py})_4\text{F}_2$  octahedra linked through  $\text{H}-\text{O}-\text{H}\cdots\text{F}$  and  $\text{H}-\text{O}-\text{H}\cdots\text{O}$  hydrogen bonding interactions. Single crystals were grown from a  $(\text{HF})_x \cdot \text{pyridine}/\text{pyridine}/\text{water}$  solution.

**Keywords:** Crystal structure; Nickel complexes; Hexafluoro complexes; Hexahydrate complexes

## 1. Background

In solid state chemistry a large number of preparative methods exist. By far the most common is direct reaction of components. To grow single crystals a variety of techniques can be employed, including fluxes, vapor phase transport, and hydro(solvato)thermal methods [1–4]. Employing the latter technique and subcritical conditions, we are studying the dissolution of transition metal oxides in a variety of solvent mixtures such as  $(\text{HF})_x \cdot \text{pyridine}$ . This non-aqueous solvent has emerged [5] as a useful and practical alternative to water and hydroxide systems.  $(\text{HF})_x \cdot \text{pyridine}$  (70 wt.% HF) is an anhydrous source of hydrofluoric acid, which when combined with water, gives rise to the following reaction [6]:



Using transition metal oxides as starting materials and nucleophilic  $\text{HF}_2^-$  we have been able to grow large crystals of new metal fluorides containing neutral or ionic molecular species, clusters and extended structures.

## 2. Introduction

The syntheses, structures and infrared and electronic spectroscopy of three new hexafluoro-hexahydrates  $[\text{Ni}(\text{H}_2\text{O})_6]^{2+} [\text{MF}_6]^{2-}$  ( $\text{M} = \text{Ti}, \text{Zr}, \text{Hf}$ ), and a new fluoro-hydrate nickel species  $\text{Ni}_3(\text{py})_{12}\text{F}_6 \cdot 7\text{H}_2\text{O}$  are reported.  $[\text{Ni}(\text{H}_2\text{O})_6]^{2+} [\text{MF}_6]^{2-}$  ( $\text{M} = \text{Ti}, \text{Zr}, \text{Hf}$ ) are isostructural to the series  $[\text{M}^{\text{II}}(\text{H}_2\text{O})_6]^{2+} [\text{M}^{\text{IV}}\text{F}_6]^{2-}$ , where  $\text{M}^{\text{II}}$  is Mg, Mn, Fe, Co, Ni or Zn and  $\text{M}^{\text{IV}}$  is Si, Ge, Sn, Ti or Zr (see Table 1) [7–10]. The divalent metal is coordinated by six water molecules, with the tetravalent metal surrounded by six fluorides forming nearly regular octahedra. The roughly spherical cations and anions pack in a distorted pseudo-CsCl type structure.  $[\text{M}^{\text{II}}(\text{H}_2\text{O})_6]^{2+} [\text{M}^{\text{IV}}\text{F}_6]^{2-}$  are isotypic with or closely related to Pauling's  $\text{NiSnCl}_6 \cdot 6\text{H}_2\text{O}$  [11].  $\text{NiSnCl}_6 \cdot 6\text{H}_2\text{O}$  crystallizes in space group  $R\bar{3}$  with the nickel and tin atoms, coordinated by water and chloride, respectively, arranged in nearly regular octahedra. Ray et al. described the crystal structures of  $\text{CoSiF}_6 \cdot 6\text{H}_2\text{O}$ ,  $\text{NiSiF}_6 \cdot 6\text{H}_2\text{O}$  and  $\text{ZnSiF}_6 \cdot 6\text{H}_2\text{O}$  to be in  $R\bar{3}$ , but with disorder in the fluorine atoms between two positions unrelated by symmetry [7]. Hamilton, using neutron diffraction, determined the space group of  $\text{FeSiF}_6 \cdot 6\text{H}_2\text{O}$  to be  $R\bar{3}m$  [12]. He postulated that a simple static disorder involving rotation

$\star$  This paper is dedicated to Professor F. Basolo.

$\star$  Corresponding author.

Table 1  
Isostructural compounds of  $[\text{Ni}(\text{H}_2\text{O})_6][\text{MF}_6]$  ( $M = \text{Ti, Zr, Hf}$ )

	$a$ (Å)	$c$ (Å)
$[\text{Mg}(\text{H}_2\text{O})_6][\text{SiF}_6]^a$	9.56	9.89
$[\text{Mn}(\text{H}_2\text{O})_6][\text{SiF}_6]^a$	9.66	9.75
$[\text{Fe}(\text{H}_2\text{O})_6][\text{SiF}_6]^a$	9.62	9.68
$[\text{Ni}(\text{H}_2\text{O})_6][\text{SiF}_6]^b$	9.363(3)	9.730(4)
$[\text{Zn}(\text{H}_2\text{O})_6][\text{SiF}_6]^b$	9.363(3)	9.690(5)
$[\text{Co}(\text{H}_2\text{O})_6][\text{SiF}_6]^b$	9.366(2)	9.730(4)
$[\text{Mg}(\text{H}_2\text{O})_6][\text{TiF}_6]^a$	9.77	9.85
$[\text{Zn}(\text{H}_2\text{O})_6][\text{TiF}_6]^a$	9.55	9.88
$[\text{Zn}(\text{H}_2\text{O})_6][\text{ZrF}_6]^a$	9.77	10.11
$[\text{Mg}(\text{H}_2\text{O})_6][\text{SnF}_6]^a$	9.77	10.02
$[\text{Zn}(\text{H}_2\text{O})_6][\text{SnF}_6]^a$	9.71	10.19
$[\text{Ni}(\text{H}_2\text{O})_6][\text{SnF}_6]^a$	10.65	10.76
$[\text{Ni}(\text{H}_2\text{O})_6][\text{GeF}_6]^c$	9.443(1)	9.770(1)
$[\text{Ni}(\text{H}_2\text{O})_6][\text{TiF}_6]$	9.489(4)	9.764(7)
$[\text{Ni}(\text{H}_2\text{O})_6][\text{ZrF}_6]$	9.727(2)	10.051(3)
$[\text{Ni}(\text{H}_2\text{O})_6][\text{HfF}_6]$	9.724(3)	10.028(4)

<sup>a</sup> Lattice parameters from Ref. [11].

<sup>b</sup> Lattice parameters from Ref. [7].

<sup>c</sup> Lattice parameters from Ref. [8].

around the three-fold axis of each cation,  $\text{Fe}^{2+}$  and  $\text{Si}^{4+}$ , was needed to explain the  $R\bar{3}m$  symmetry. All of the above fluorides were synthesized from a combination of the divalent metal carbonate with either fluorosililic, fluorogermanic, tin fluoride, fluorotitanic acid or zirconium fluoride. The products were crystallized from aqueous solution.

The structure and synthesis of  $\text{Ni}_3(\text{py})_{12}\text{F}_6 \cdot 7\text{H}_2\text{O}$ , which is related to the series  $\text{M}^{\text{II}}(\text{pyridine})_4\text{X}_2$  where  $\text{M}^{\text{II}} = \text{Fe, Co, Ni}$ , and  $\text{X} = \text{Cl, Br, I}$  [13–17], is also reported. In all cases, the halide ions are *trans*, with the  $\text{X}-\text{M}^{\text{II}}-\text{X}$  bond angle of  $180^\circ$ , while the pyridine rings are in pseudo-square planar configuration. A hydrated form of the iron (II)-pyridine complex,  $\text{Fe}(\text{py})_4\text{Cl}_2 \cdot \text{H}_2\text{O}$ , has also been reported [14]. The water molecules in  $\text{Fe}(\text{py})_4\text{Cl}_2 \cdot \text{H}_2\text{O}$  bridge with hydrogen bonds between octahedra. The  $\text{M}^{\text{II}}(\text{py})_4\text{X}_2$  compounds were synthesized by dissolving the hydrated transition metal halide in a 50% (vol./vol.) pyridine/methanol solution [15]. Single crystals were grown by slow evaporation of the solvent.

### 3. Experimental

#### 3.1. Synthesis

$[\text{Ni}(\text{H}_2\text{O})_6]^{2+}[\text{MF}_6]^{2-}$  ( $M = \text{Ti, Zr, Hf}$ ) were synthesized by dissolving equimolar amounts of the respective oxides in aq. hydrofluoric acid (40%, Alfa) in a Teflon beaker. Large green crystals were obtained upon slow evaporation of the solvent.

$\text{Ni}_3(\text{py})_{12}\text{F}_6 \cdot 7\text{H}_2\text{O}$  was synthesized by adding  $3.7 \times 10^{-2}$  g ( $5 \times 10^{-4}$  mol) of NiO (99.99%, Aldrich) to  $3.4 \times 10^{-1}$  g ( $1 \times 10^{-3}$  mol) of  $(\text{HF})_x \cdot \text{pyridine}$  (pyridinium poly(hydrogen fluoride), 70 wt.% HF, Aldrich),  $7.9 \times 10^{-1}$  g ( $1 \times 10^{-2}$  mol) pyridine (99.8% anhydrous, Aldrich), and

$9.0 \times 10^{-2}$  g ( $5 \times 10^{-4}$  mol)  $\text{H}_2\text{O}$ . The resulting mixture was placed in a Teflon pouch [18]. The pouch was sealed, placed in a 2000 ml autoclave (Parr) filled with 600 ml of water, heated for 24 h at  $150^\circ\text{C}$ , cooled over 24 h to r.t., and removed from the autoclave. Upon removal, a clear light blue solution was observed in the pouch. The pouch was allowed to stand undisturbed; light blue crystals which formed within two days were subsequently determined to be  $\text{Ni}_3(\text{py})_{12}\text{F}_6 \cdot 7\text{H}_2\text{O}$ . The pouch was then opened in air and the crystals recovered by filtration.

#### 3.2. Spectroscopy

Mid-IR ( $400\text{--}4000\text{ cm}^{-1}$ ) spectra were collected using a Bomem MB-100 Fourier transform IR spectrometer equipped with a DTGS detector operating at a resolution of  $1\text{ cm}^{-1}$ . Spectra were collected as Nujol mulls using KBr plates.

Visible electronic absorption spectra were recorded on a Hewlett-Packard 8425A diode array spectrophotometer. Each sample was prepared by dissolving the compound in distilled water.

#### 3.3. Crystallography

All single crystal data collections and structure refinements were performed on an Enraf-Nonius CAD-4 diffractometer with graphite monochromated Mo  $K\alpha$  radiation. All calculations were performed using the TEXSAN [19] crystallographic software package of Molecular Structure Corporation. The quality of each of the crystals was determined by Weissenberg photography. 25 well-centered reflections were used to determine the unit cells. On the basis of systematic absences and successful solution and refinement of the structures, the space group was determined to be  $R\bar{3}$  (No. 148) for the  $[\text{Ni}(\text{H}_2\text{O})_6]^{2+}[\text{MF}_6]^{2-}$  ( $M = \text{Ti, Zr, Hf}$ ) salts, and  $I2/a$  (No. 15) for  $\text{Ni}_3(\text{py})_{12}\text{F}_6 \cdot 7\text{H}_2\text{O}$ . In all cases the metal positions were found by direct methods [20,21], while the remaining non-hydrogen atom positions were located from difference Fourier maps. Neutral atom scattering factors were used in all calculations. All non-hydrogen atoms were refined anisotropically.

##### 3.3.1. $[\text{Ni}(\text{H}_2\text{O})_6][\text{TiF}_6]$

A  $0.24 \times 0.24 \times 0.43$  mm crystal was used for indexing and intensity data collection. Of the 842 unique reflections collected, 346 were observed under the criterion of  $I \geq 3.00\sigma(I)$ . An analytical absorption correction was applied resulting in transmission factors ranging from 0.27–0.68. The final cycles of refinement, including those for the atomic positions and anisotropic thermal parameters (24 variables), converged with  $R = 0.083$  and  $R_w = 0.133$ . A secondary extinction correction was applied and refined to a value of  $2.117 \times 10^{-6}$ . The maximum and minimum peaks on the final difference Fourier map corresponded to 1.25 and  $-1.48\text{ e \AA}^{-3}$  respec-

Table 2  
Crystal data for  $[\text{Ni}(\text{H}_2\text{O})_6][\text{TiF}_6]$ ,  $[\text{Ni}(\text{H}_2\text{O})_6][\text{ZrF}_6]$  and  $[\text{Ni}(\text{H}_2\text{O})_6][\text{HfF}_6]$

Formula	$[\text{Ni}(\text{H}_2\text{O})_6][\text{TiF}_6]$	$[\text{Ni}(\text{H}_2\text{O})_6][\text{ZrF}_6]$	$[\text{Ni}(\text{H}_2\text{O})_6][\text{HfF}_6]$
Formula weight	328.68	372.03	459.27
Crystal system	trigonal	trigonal	trigonal
Space group	$R\bar{3}$ (No. 148)	$R\bar{3}$ (No. 148)	$R\bar{3}$ (No. 148)
<i>a</i> (Å)	9.489(4)	9.727(2)	9.724(3)
<i>b</i> (Å)	9.489(4)	9.727(2)	9.724(3)
<i>c</i> (Å)	9.764(7)	10.051(3)	10.028(4)
<i>V</i> (Å <sup>3</sup> )	761(1)	823.6(6)	821.2(8)
<i>Z</i>	3	3	3
<i>F</i> (000)	492	546	642
<i>h, k, l</i> collected	$-h, -k, \pm l$	$+h, +k, \pm l$	$-h, -k, \pm l$
Temperature (°C)	-120	-120	-120
<i>D</i> <sub>calc</sub> (g/ml)	2.151	2.250	2.786
<i>D</i> <sub>obs</sub> (g/ml) <sup>a</sup>	2.03(1)	2.22(5)	2.68(3)
Radiation (Å)		Mo Kα (graphite-monochromated) λ = 0.71069	
μ (cm <sup>-1</sup> )	27.36	27.44	112.08
Transmission factors (min., max.)	0.27, 0.68	0.50, 0.72	0.10, 0.17
Reflections recorded	1010	1880	1417
2θ (max.) (°)	54	60	54
Unique reflections	842	1617	1205
Observed reflections ( <i>I</i> ≥ 3.00σ( <i>I</i> ))	346	495	403
<i>R</i> <sup>b</sup>	0.083	0.038	0.034
<i>R</i> <sub>w</sub> <sup>c</sup>	0.133	0.090	0.047

<sup>a</sup> Density measured at 24 °C by flotation method pycnometry.

<sup>b</sup>  $R = \sum \|F_o\| - |F_c| / \sum \|F_o\|$ .

<sup>c</sup>  $R_w = \sum w(\|F_o\| - |F_c|)^2 / \sum w(\|F_o\|^2)$ <sup>1/2</sup>;  $w = 1/\sigma^2(F_o) = 4F_o/\sigma^2(F_o^2)$ ;  $\sigma^2(F_o^2) = S^2(C + R^2B) + (pF_o^2)^2/Lp^2$ . *S* = scan rate, *C* = total integrated peak count, *R* = ratio of scan time to background counting time, *B* = total background count, *Lp* = Lorentz-polarization factor, *p* = *p* factor.

tively. No meaningful electron densities could be found for the hydrogen atoms.

### 3.3.2. $[\text{Ni}(\text{H}_2\text{O})_6][\text{ZrF}_6]$

A  $0.18 \times 0.24 \times 0.30$  mm crystal was used for indexing and intensity data collection. Of the 1617 unique reflections collected, 495 were observed under the criterion of  $I \geq 3.00\sigma(I)$ . An analytical absorption correction was applied resulting in transmission factors ranging from 0.50–0.72. The final cycles of refinement, including those for the atomic positions and anisotropic thermal parameters (24 variables), converged with  $R = 0.038$  and  $R_w = 0.090$ . A secondary extinction correction was applied and refined to a value of  $3.555 \times 10^{-6}$ . The maximum and minimum peaks on the final difference Fourier map corresponded to 1.60 and  $-2.19 \text{ e } \text{Å}^{-3}$  respectively. No meaningful electron densities could be found for the hydrogen atoms.

### 3.3.3. $[\text{Ni}(\text{H}_2\text{O})_6][\text{HfF}_6]$

A  $0.21 \times 0.21 \times 0.36$  mm crystal was used for indexing and intensity data collection. Of the 1205 unique reflections collected, 403 were observed under the criterion of  $I \geq 3.00\sigma(I)$ . An analytical absorption correction was applied resulting in transmission factors ranging from 0.10–0.17. The final cycles of refinement, including those for the atomic positions and anisotropic thermal parameters (24 variables), converged with  $R = 0.034$  and  $R_w = 0.047$ . A secondary extinction correction was applied and refined to a value of  $1.269 \times 10^{-5}$ .

The maximum and minimum peaks on the final difference Fourier map corresponded to 1.18 and  $-1.68 \text{ e } \text{Å}^{-3}$  respectively. No meaningful electron densities could be found for the hydrogen atoms.

Relevant crystal data for  $[\text{Ni}(\text{H}_2\text{O})_6]^{2+}[\text{MF}_6]^{2-}$  (*M* = Ti, Zr, Hf) are given in Table 2, with atomic coordinates and bond distances and angles given in Tables 3 and 4, respectively.

### 3.3.4. $\text{Ni}_3(\text{py})_{12}\text{F}_6 \cdot 7\text{H}_2\text{O}$

A  $0.20 \times 0.25 \times 0.14$  mm crystal was used for indexing and intensity data collection. Of the 9191 reflections collected, 5766 were unique ( $R_{\text{int}} = 0.046$ ). 2268 reflections were observed under the criterion of  $I \geq 3.00\sigma(I)$ . An analytical absorption correction was applied, resulting in transmission factors ranging from 0.83–0.88.

The pyridinyl hydrogens were placed in idealized positions, while the lattice water hydrogens were neither placed in calculated positions nor located in the final difference Fourier map. The final refinement (400 variables) converged with  $R = 0.047$  and  $R_w = 0.046$ . A secondary extinction correction was applied and refined to a value of  $8.438 \times 10^{-6}$ . The maximum and minimum peaks on the final difference Fourier map corresponded to 0.26 and  $-0.37 \text{ e } \text{Å}^{-3}$  respectively. Relevant crystal data for  $\text{Ni}_3(\text{py})_{12}\text{F}_6 \cdot 7\text{H}_2\text{O}$  are given in Table 5, with atomic coordinates and bond distances and angles given in Tables 6 and 7, respectively.

Table 3  
Atomic coordinates for  $[\text{Ni}(\text{H}_2\text{O})_6][\text{MF}_6]$  ( $M = \text{Ti}, \text{Zr}, \text{Hf}$ )<sup>a</sup>

Atom	Site	x	y	z	mult	$B_{\text{eq}} (\text{Å}^2)$ <sup>b</sup>
$[\text{Ni}(\text{H}_2\text{O})_6][\text{TiF}_6]$						
Ti	3a	0.0000	0.0000	0.0000	0.1667	1.6(1)
Ni	3b	0.0000	0.0000	0.5000	0.1667	1.25(6)
F	18f	0.067(1)	0.1764(6)	0.1066(5)	1.0000	4.1(3)
O	18f	0.1775(6)	0.0005(7)	0.3823(5)	1.0000	1.9(2)
$[\text{Ni}(\text{H}_2\text{O})_6][\text{ZrF}_6]$						
Zr	3a	0.0000	0.0000	0.0000	0.1667	0.80(3)
Ni	3b	0.0000	0.0000	0.5000	0.1667	0.95(4)
F	18f	0.0440(4)	0.1849(4)	0.1153(3)	1.0000	2.1(1)
O	18f	0.1709(4)	-0.0069(5)	0.3860(3)	1.0000	1.5(1)
$[\text{Ni}(\text{H}_2\text{O})_6][\text{HfF}_6]$						
Hf	3a	0.0000	0.0000	0.0000	0.1667	0.86(3)
Ni	3b	0.0000	0.0000	0.5000	0.1667	0.96(5)
F	18f	0.0445(6)	0.1838(5)	0.1150(4)	1.0000	2.3(1)
O	18f	0.1720(6)	-0.0058(6)	0.3864(5)	1.0000	1.6(1)

<sup>a</sup> Numbers in parentheses are standard deviations in the last significant figure.

<sup>b</sup>  $B_{\text{eq}} = (8/3)\pi^2(U_{11}(aa^*)^2 + U_{22}(bb^*)^2 + U_{33}(cc^*)^2 + 2U_{12}aa^*bb^* \cos \gamma + 2U_{13}aa^*cc^* \cos \beta + 2U_{23}bb^*cc^* \cos \alpha)$ .

Table 4  
Selected interatomic distances (Å) and angles (°)

Atoms	$[\text{Ni}(\text{H}_2\text{O})_6][\text{TiF}_6]$	$[\text{Ni}(\text{H}_2\text{O})_6][\text{ZrF}_6]$	$[\text{Ni}(\text{H}_2\text{O})_6][\text{HfF}_6]$			
<b>Distances</b>						
$M^{\text{II}}-\text{O}$	Ni-O	2.038(5)	Ni-O	2.047(3)	Ni-O	2.047(5)
$M^{\text{IV}}-\text{F}$	Ti-F	1.796(5)	Zr-F	1.997(3)	Hf-F	1.985(4)
$M^{\text{II}}-M^{\text{IV}}$	Ni-Ti	4.88(1)	Ni-Zr	5.02(1)	Ni-Hf	5.01(1)
O-F	O-F	2.737(7)	O-F	2.735(6)	O-F	2.735(6)
<b>Angles</b>						
	O(1)-Ni-O(1)*	88.7(2)	O(1)-Ni-O(1)*	88.3(1)	O(1)-Ni-O(1)*	88.0(2)
	O(1)*-Ni-O(1)**	91.3(2)	O(1)*-Ni-O(1)**	91.7(1)	O(1)*-Ni-O(1)**	92.0(2)
	F(1)-Ti-F(1)*	89.8(2)	F(1)-Zr-F(1)*	89.7(1)	F(1)-Hf-F(1)*	89.6(2)
	F(1)*-Ti-F(1)**	90.2(2)	F(1)*-Zr-F(1)**	90.3(1)	F(1)*-Hf-F(1)**	90.4(2)

Single starred atoms indicate equatorial contacts.

Double starred atoms indicate apical contacts.

#### 4. Results and discussion

Similar to the series  $[\text{M}^{\text{II}}(\text{H}_2\text{O})_6]^{2+}[\text{M}^{\text{IV}}\text{F}_6]^{2-}$ ,  $[\text{Ni}(\text{H}_2\text{O})_6]^{2+}[\text{MF}_6]^{2-}$  ( $M = \text{Ti}, \text{Zr}, \text{Hf}$ ) are isostructural to  $\text{NiSnCl}_6 \cdot 6\text{H}_2\text{O}$  [11]. These compounds crystallize in a distorted pseudo-CsCl type packing as salts with  $[\text{Ni}(\text{H}_2\text{O})_6]^{2+}$  octahedra as the cations and  $[\text{MF}_6]^{2-}$  octahedra as the anions. A polyhedral representation is shown in Fig. 1 from which the trigonal cell is easily observed. The cations and anions alternate positions in the  $b$ - $c$  plane as well as down the  $a$ -axis. In addition, hydrogen bonding occurs via  $\text{H}-\text{O}-\text{H} \cdots \text{F}$  interactions. The O-F distances given in Table 3 are consistent with other hydrogen-bonded complexes [12,22]. A comparison of lattice volumes beautifully illus-

trates the behavior of this  $M^{\text{IV}}$  triad. Owing to the larger  $\text{Zr}^{4+}$  cation compared to  $\text{Ti}^{4+}$  we observe a substantial increase in volume between  $[\text{Ni}(\text{H}_2\text{O})_6][\text{TiF}_6]$  and  $[\text{Ni}(\text{H}_2\text{O})_6][\text{ZrF}_6]$ . Additionally, comparing  $[\text{Ni}(\text{H}_2\text{O})_6][\text{ZrF}_6]$  and  $[\text{Ni}(\text{H}_2\text{O})_6][\text{HfF}_6]$  we observe a slight decrease in volume because of the lanthanide contraction (see Table 2).

$\text{Ni}_3(\text{py})_{12}\text{F}_6 \cdot 7\text{H}_2\text{O}$  may be described as discrete  $\text{Ni}(\text{py})_4\text{F}_2$  octahedra which have crystallized to form a network of interlayer hydrogen bonds with lattice water molecules. The compositional variation of the lattice water observed in  $\text{Ni}_3(\text{py})_{12}\text{F}_6 \cdot 7\text{H}_2\text{O}$  is an interesting feature of the structure. A crystal packing diagram is shown in Fig. 2. The  $\text{Ni}(\text{py})_4\text{F}_2$  molecules pack in two distinct layers, **a** and **b**, with six layers per unit cell. The layer repeat sequence may

Table 5  
Crystal data for  $\text{Ni}_3(\text{py})_{12}\text{F}_6 \cdot 7\text{H}_2\text{O}$

Formula	$\text{Ni}_3(\text{py})_{12}\text{F}_6 \cdot 7\text{H}_2\text{O}$
Formula weight	1364.33
Crystal system	monoclinic
Space group	$I2/a$ (No. 15)
$a$ (Å)	16.117(4)
$b$ (Å)	8.529(3)
$c$ (Å)	46.220(7)
$\beta$ (°)	92.46(2)
$V$ (Å <sup>3</sup> )	6348(5)
$Z$	4
$F(000)$	2856
$h, k, l$ collected	$\pm h, \pm k, -l$
Temperature (°C)	-120
$D_{\text{calc}}$ (g/ml)	1.428
$D_{\text{obs}}$ (g/ml) <sup>a</sup>	1.43(1)
Radiation (Å)	Mo $K\alpha$ (graphite-monochromated)
	$\lambda = 0.71069$
$\mu$ (cm <sup>-1</sup> )	9.6
Transmission factors (min., max.)	0.83, 0.88
Reflections recorded	9191
$2\theta$ (max.) (°)	54
Unique reflections	5766
Observed reflections ( $I \geq 3.00\sigma(I)$ )	2268
$R$ <sup>b</sup>	0.047
$R_w$ <sup>c</sup>	0.046

<sup>a</sup> Density measured at 24 °C by flotation method pycnometry.

<sup>b</sup>  $R = \sum \|F_o| - |F_c|\| / \sum |F_o|$ .

<sup>c</sup>  $R_w = \sum w(\|F_o| - |F_c|\|^2 / \sum w(|F_o|^2))^{1/2}$ ;  $w = 1/\sigma^2(F_o) = 4F_o/\sigma^2(F_o^2)$ ;  $\sigma^2(F_o^2) = S^2(C + R^2B) + (pF_o^2)^2/Lp^2$ .  $S$  = scan rate,  $C$  = total integrated peak count,  $R$  = ratio of scan time to background counting time,  $B$  = total background count,  $Lp$  = Lorentz-polarization factor,  $p$  =  $p$  factor.

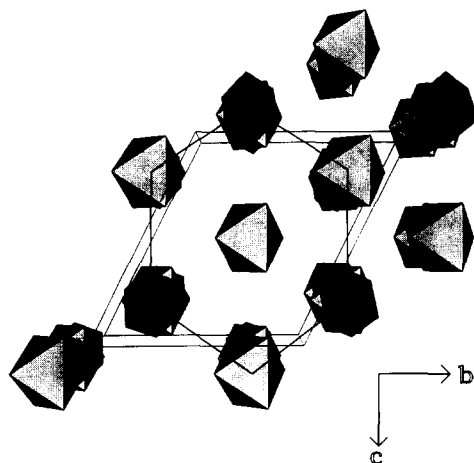


Fig. 1. Polyhedral representation of  $[\text{Ni}(\text{H}_2\text{O})_6]^{2+} [\text{MF}_6]^{2-}$  showing the trigonal unit cell and the hexagonal pattern. Light shaded polyhedra are  $[\text{Ni}(\text{H}_2\text{O})_6]^{2+}$  and dark shaded polyhedra are  $[\text{MF}_6]^{2-}$ . Note the alternation of polyhedra on the  $b$ - $c$  plane and down the  $a$ -axis.

be described as  $(\text{aba})_2$ , with two distinct types of interlayer environments. Between layers **a** and **b** three  $\text{H}_2\text{O}$  molecules exist for every two  $\text{Ni}(\text{py})_4\text{F}_2$  molecules, while between the **a** layers two  $\text{H}_2\text{O}$  molecules exist for every  $\text{Ni}(\text{py})_4\text{F}_2$  molecule. Although the primary coordination environment of nickel in each  $\text{Ni}(\text{py})_4\text{F}_2$  molecule is identical, the secondary coordination shell is different. This difference is due to the

unequal number of water molecules between layers **a** and **b** and between the **a** layers. Between layers **a** and **b** hydrogen bonding occurs by  $\text{O}-\text{H}\cdots\text{F}$  interactions; however, between the **a** layers hydrogen bonding occurs by both  $\text{O}-\text{H}\cdots\text{F}$  and  $\text{O}-\text{H}\cdots\text{O}$  interactions. As seen in Fig. 3 the combination of both types of hydrogen bonding,  $\text{O}-\text{H}\cdots\text{F}$  and  $\text{O}-\text{H}\cdots\text{O}$ , link the **a** layers throughout the structure. The IR spectrum of  $\text{Ni}_3(\text{py})_{12}\text{F}_6 \cdot 7\text{H}_2\text{O}$  was unexceptional except for three hydrogen bonding stretches at 1914, 2370 and 2485  $\text{cm}^{-1}$ .

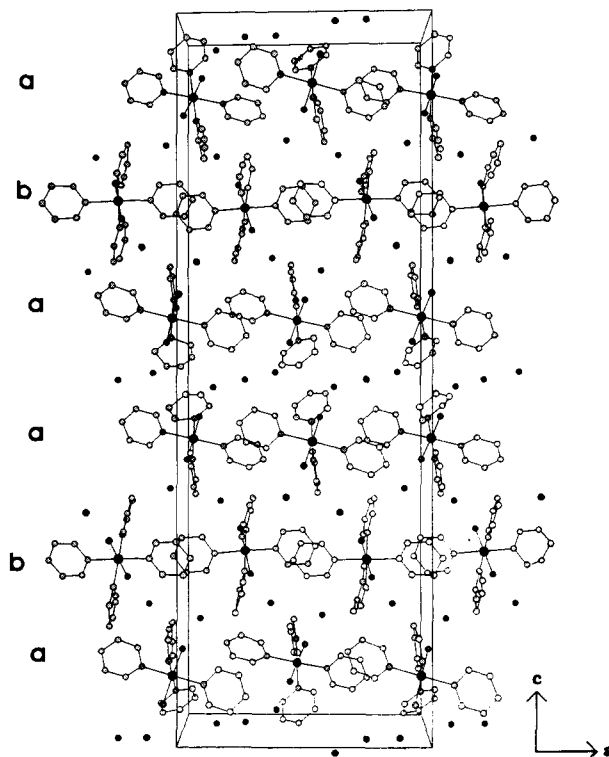


Fig. 2. Crystal packing diagram of  $\text{Ni}_3(\text{py})_{12}\text{F}_6 \cdot 7\text{H}_2\text{O}$ . Layers marked by **a** and **b** are described in text.

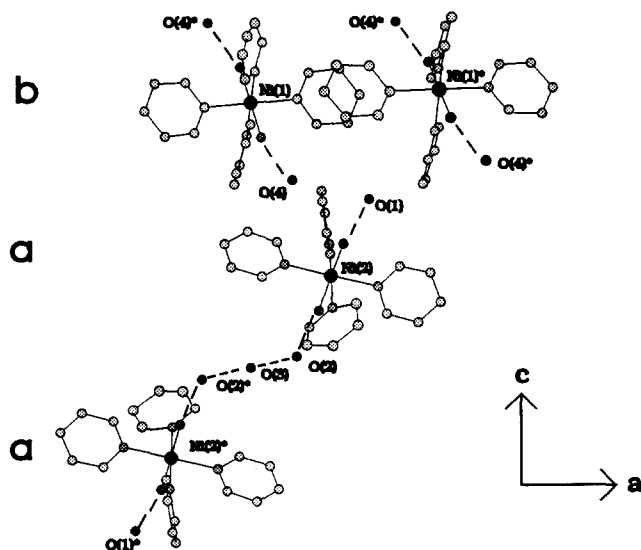


Fig. 3. Representation of  $\text{Ni}_3(\text{py})_{12}\text{F}_6 \cdot 7\text{H}_2\text{O}$  with dashed lines indicating hydrogen bonding. Starred atoms indicate symmetry equivalent atoms.

Table 6  
Atomic coordinates and  $B_{\text{eq}}$  for  $\text{Ni}_3(\text{py})_{12}\text{F}_6 \cdot 7\text{H}_2\text{O}^a$

Atom	Site	x	y	z	$B_{\text{eq}}^b$ ( $\text{\AA}^2$ )
Ni(1)	c	3/4	1/4	1/4	1.43(4)
Ni(2)	f	0.53161(4)	0.2559(1)	0.08685(1)	1.43(3)
F(1)	f	0.7744(3)	0.0804(5)	0.27948(7)	2.1(2)
F(2)	f	0.4977(3)	0.4031(5)	0.11812(7)	1.8(1)
F(3)	f	0.5632(3)	0.1126(5)	0.05383(7)	2.4(2)
O(1)	f	0.4276(3)	0.4168(8)	0.16151(9)	2.8(2)
O(2)	f	0.6225(4)	0.0639(8)	0.01074(9)	3.0(2)
O(3)	e	3/4	0.268(3)	0	7.7(7)
O(4)	f	0.6403(3)	0.4892(7)	0.18121(8)	2.3(2)
N(1)	f	0.6584(4)	0.2974(7)	0.0982(1)	1.9(2)
N(2)	f	0.4049(4)	0.2065(7)	0.0764(1)	1.8(2)
N(3)	f	0.5277(4)	0.4472(8)	0.0577(1)	2.0(2)
N(4)	f	0.5370(4)	0.0611(7)	0.1150(1)	1.9(2)
N(5)	f	0.6224(4)	0.1936(7)	0.2520(1)	1.8(2)
N(6)	f	0.7563(4)	0.0784(8)	0.2164(1)	1.7(2)
C(1)	f	0.6793(4)	0.3918(8)	0.1206(1)	2.0(2)
C(2)	f	0.7628(4)	0.412(1)	0.1307(1)	2.4(3)
C(3)	f	0.8244(4)	0.329(1)	0.1174(2)	2.7(3)
C(4)	f	0.8027(4)	0.230(1)	0.0948(2)	2.8(3)
C(5)	f	0.7190(4)	0.2176(8)	0.0857(1)	2.2(3)
C(6)	f	0.3805(5)	0.148(1)	0.0509(1)	2.6(3)
C(7)	f	0.2972(5)	0.124(1)	0.0425(1)	3.1(3)
C(8)	f	0.2362(5)	0.160(1)	0.0618(2)	3.1(3)
C(9)	f	0.2638(5)	0.217(1)	0.0887(2)	3.4(4)
C(10)	f	0.3463(5)	0.239(1)	0.0956(1)	2.7(3)
C(11)	f	0.4639(5)	0.545(1)	0.0566(1)	2.7(3)
C(12)	f	0.4590(6)	0.675(1)	0.0386(2)	3.2(3)
C(13)	f	0.5247(6)	0.701(1)	0.0204(2)	3.4(3)
C(14)	f	0.5900(6)	0.598(1)	0.0210(2)	3.4(3)
C(15)	f	0.5905(5)	0.472(1)	0.0397(1)	2.6(3)
C(16)	f	0.5477(5)	0.079(1)	0.1440(1)	2.7(3)
C(17)	f	0.5555(7)	-0.050(1)	0.1623(1)	3.8(4)
C(18)	f	0.5534(6)	-0.198(1)	0.1509(2)	3.6(4)
C(19)	f	0.5416(4)	-0.2158(8)	0.1215(2)	2.5(3)
C(20)	f	0.5336(4)	-0.085(1)	0.1044(1)	2.0(2)
C(21)	f	0.5911(5)	0.127(1)	0.2756(1)	2.5(3)
C(22)	f	0.5083(6)	0.090(1)	0.2778(2)	3.1(3)
C(23)	f	0.4536(4)	0.124(1)	0.2544(2)	3.1(3)
C(24)	f	0.4856(5)	0.187(1)	0.2296(2)	3.3(3)
C(25)	f	0.5702(5)	0.2220(9)	0.2294(1)	2.3(3)
C(26)	f	0.7447(5)	-0.071(1)	0.2226(1)	2.3(3)
C(27)	f	0.7535(6)	-0.190(1)	0.2032(2)	3.3(3)
C(28)	f	0.7784(7)	-0.155(1)	0.1761(2)	3.6(4)
C(29)	f	0.7887(8)	-0.000(1)	0.1690(2)	4.1(4)
C(30)	f	0.7770(6)	0.114(1)	0.1893(1)	3.1(3)
H(1)	f	0.6367	0.4469	0.1299	2.4
H(2)	f	0.7763	0.4810	0.1463	2.9
H(3)	f	0.8810	0.3398	0.1238	3.2
H(4)	f	0.8440	0.1716	0.0855	3.3
H(5)	f	0.7045	0.1500	0.0700	2.7
H(6)	f	0.4218	0.1211	0.0377	3.1
H(7)	f	0.2823	0.0840	0.0239	3.6
H(8)	f	0.1788	0.1462	0.0569	3.7
H(9)	f	0.2242	0.2416	0.1027	4.1
H(10)	f	0.3629	0.2784	0.1142	3.3
H(11)	f	0.4192	0.5259	0.0689	3.3
H(12)	f	0.4126	0.7431	0.0385	3.9
H(13)	f	0.5239	0.7898	0.0079	4.0
H(14)	f	0.6348	0.6141	0.0086	4.0
H(15)	f	0.6359	0.4003	0.0400	3.1
H(16)	f	0.5497	0.1812	0.1521	3.3
H(17)	f	0.5626	-0.0358	0.1827	4.6
H(18)	f	0.5598	-0.2866	0.1631	4.3

(continued)

Table 6 (continued)

Atom	Site	x	y	z	$B_{\text{eq}}^b$ ( $\text{\AA}^2$ )
H(19)	f	0.5392	-0.3177	0.1132	3.0
H(20)	f	0.5252	-0.0986	0.0840	2.4
H(21)	f	0.6281	0.1032	0.2916	3.0
H(22)	f	0.4888	0.0426	0.2948	3.7
H(23)	f	0.3958	0.1032	0.2554	3.7
H(24)	f	0.4504	0.2071	0.2129	3.9
H(25)	f	0.5916	0.2677	0.2126	2.7
H(26)	f	0.7293	-0.0973	0.2416	2.8
H(27)	f	0.7426	-0.2952	0.2085	3.9
H(28)	f	0.7883	-0.2361	0.1625	4.3
H(29)	f	0.8037	0.0279	0.1500	4.9
H(30)	f	0.7837	0.2212	0.1841	3.7

<sup>a</sup> Numbers in parentheses are standard deviations in the last significant figure.

<sup>b</sup>  $B_{\text{eq}} = (8/3)\pi^2(U_{11}(aa^*)^2 + U_{22}(bb^*)^2 + U_{33}(cc^*)^2 + 2U_{12}aa^*bb^* \cos \gamma + 2U_{13}aa^*cc^* \cos \beta + 2U_{23}bb^*cc^* \cos \alpha)$ .

Table 7

Selected intramolecular bond distances ( $\text{\AA}$ ) and angles ( $^\circ$ ) for  $\text{Ni}_3(\text{py})_{12}\text{F}_6 \cdot 7\text{H}_2\text{O}^a$

Ni(1)–F(1)	2.015(4)
Ni(1)–N(5)	2.118(6)
Ni(1)–N(6)	2.140(6)
Ni(2)–F(2)	2.008(3)
Ni(2)–F(3)	2.037(4)
Ni(2)–N(1)	2.118(6)
Ni(2)–N(2)	2.121(6)
Ni(2)–N(3)	2.115(6)
Ni(2)–N(4)	2.108(6)
F(1)–O(4)	2.308(6)
F(2)–O(1)	2.346(5)
F(3)–O(2)	2.284(5)
O(2)–O(3)	2.76(2)
F(1)–Ni(1)–F(1)	180.00
F(1)–Ni(1)–N(5)	88.2(2)
F(1)–Ni(1)–N(5)	91.8(2)
F(1)–Ni(1)–N(6)	89.2(2)
F(1)–Ni(1)–N(6)	90.8(2)
N(5)–Ni(1)–N(5)	180.00
N(5)–Ni(1)–N(6)	87.3(2)
N(5)–Ni(1)–N(6)	92.7(2)
N(6)–Ni(1)–N(6)	180.00
F(2)–Ni(2)–F(3)	177.5(2)
F(2)–Ni(2)–N(1)	90.3(2)
F(2)–Ni(2)–N(2)	89.9(2)
F(2)–Ni(2)–N(3)	88.6(2)
F(2)–Ni(2)–N(4)	93.1(2)
F(3)–Ni(2)–N(1)	90.9(2)
F(3)–Ni(2)–N(2)	88.9(2)
F(3)–Ni(2)–N(3)	88.6(2)
F(3)–Ni(2)–N(4)	89.1(2)
N(1)–Ni(2)–N(2)	177.8(2)
N(2)–Ni(2)–N(3)	91.8(2)
N(1)–Ni(2)–N(4)	88.0(2)
N(2)–Ni(2)–N(3)	90.4(2)
N(2)–Ni(2)–N(4)	89.8(2)
N(3)–Ni(2)–N(4)	178.3(2)

<sup>a</sup> Numbers in parentheses are standard deviations in the last significant figure.

Table 8  
Atomic distances (Å) in metal-pyridine compounds

	M–N(av.)	M–X(av.)	Ref.
Ni <sub>3</sub> (py) <sub>12</sub> F <sub>6</sub> ·7H <sub>2</sub> O	2.120(6)	2.015(4)	this work
Ni(py) <sub>4</sub> Cl <sub>2</sub>	2.121(3)	2.433(1)	13
Ni(py) <sub>4</sub> I <sub>2</sub>	2.217(7)	2.886(1)	15
Fe(py) <sub>4</sub> Cl <sub>2</sub>	2.229(6)	2.430(3)	15
Fe(py) <sub>4</sub> Cl <sub>2</sub> ·H <sub>2</sub> O	2.246(4)	2.428(2)	15
Co(py) <sub>4</sub> Cl <sub>2</sub>	2.183(4)	2.444(2)	24
Cu(py) <sub>2</sub> Cl <sub>2</sub>	2.004(5)	2.662(2)	16
Zn(py) <sub>2</sub> Cl <sub>2</sub>	2.049(6)	2.222(2)	17

Table 9  
Visible electronic absorption in Ni(II)-octahedral complexes

Complex	Bands (cm <sup>-1</sup> )	Ref.
Ni(py) <sub>4</sub> (H <sub>2</sub> O) <sub>2</sub> <sup>2+</sup>	15760, 28000	23
Ni <sub>3</sub> (py) <sub>12</sub> F <sub>6</sub> ·7H <sub>2</sub> O	15244, 25773	this work
Ni(py) <sub>4</sub> Cl <sub>2</sub>	15265, 27175	25
Ni(py) <sub>4</sub> Br <sub>2</sub>	14105, 25910	25
Ni(H <sub>2</sub> O) <sub>6</sub> MF <sub>6</sub>	13928, 25381	this work
Ni(H <sub>2</sub> O) <sub>6</sub> <sup>2+</sup>	13800, 25300	26
Ni(NH <sub>3</sub> ) <sub>6</sub> <sup>2+</sup>	17500, 28100	26

The bands at 2370 and 2485 cm<sup>-1</sup> are caused by hydrogen bonding interactions between fluorine and lattice water, while the 1914 cm<sup>-1</sup> band is the result of hydrogen bonding between lattice water molecules. The distances are given in Table 7, and compare well with other hydrogen bonded complexes [22,23].

The octahedral unit, Ni(py)<sub>4</sub>F<sub>2</sub>, is structurally similar to other M<sup>II</sup>(py)<sub>4</sub>X<sub>2</sub> compounds. A comparison of bond lengths is given in Table 8. In all cases the halide ion is *trans* with respect to the metal, with a linear X–M–X configuration. In addition, the four nitrogens are coordinated to the metal in a pseudo-square planar environment. The visible electronic absorption spectrum is typical for Ni(II)-octahedral complexes. The results, along with relevant comparisons, are listed in Table 9. The observed bands result from the spin allowed transitions in tetragonal high-spin d<sup>8</sup> systems [24]. The shift to lower frequencies from [Ni(py)<sub>4</sub>(H<sub>2</sub>O)<sub>2</sub>]<sup>2+</sup> to Ni<sub>3</sub>(py)<sub>12</sub>F<sub>6</sub>·7H<sub>2</sub>O may be rationalized by using crystal field arguments. Because aquo ligands induce a stronger crystal field than fluoride ligands (in equivalent coordination environments), absorption bands in aquo-, compared to fluoro systems occur at higher energies, which is the trend observed (see Table 9). The possibility of H<sub>2</sub>O, OH<sup>-</sup>, or O<sup>2-</sup> ligands coordinated to nickel, in Ni<sub>3</sub>(py)<sub>12</sub>F<sub>6</sub>·7H<sub>2</sub>O, in place of fluoride was considered. Because F<sup>-</sup> and O<sup>2-</sup> have similar scattering factors, these species cannot be excluded simply by crystallography. However, the electronic spectrum of Ni<sub>3</sub>(py)<sub>12</sub>F<sub>6</sub>·7H<sub>2</sub>O is consistent with coordinated fluoride.

## 5. Supplementary material

Listings of the anisotropic thermal parameters, intermolecular contacts, and structure factor tables are available from the authors upon request.

## Acknowledgements

The authors gratefully acknowledge support from the National Science Foundation, Solid State Chemistry, Contract DMR-9412971. The authors acknowledge Rachel Bain for help in collecting the IR spectra and Alan Allgeier for assistance in collecting the electronic spectra.

## References

- [1] A.R. West, *Solid State Chemistry and its Applications*, Wiley, Chichester, UK, 1984.
- [2] A. Wold and K. Dwight, *Solid State Chemistry*, Chapman and Hall, New York, 1993.
- [3] H. Schäfer, *Angew. Chem. Int. Ed. Engl.*, 10 (1971) 43.
- [4] R.A. Laudise in F.A. Cotton (ed.), *Progress in Inorganic Chemistry*, Vol. 3, Wiley, Chichester, UK, 1962, Ch. 1.
- [5] A. Kuperman, S. Nadimi, S. Oliver, G.A. Ozin, J.M. Garces and M.M. Olken, *Nature (London)*, 365 (1993) 239.
- [6] T.C. Waddington, *Non-Aqueous Solvent Systems*, Academic Press, New York, 1965.
- [7] S. Ray, A. Zalkin and D.H. Templeton, *Acta Crystallogr., Sect. B*, 29 (1973) 2741.
- [8] B.F. Hoskins and A. Linden, *Aust. J. Chem.*, 40 (1987) 565.
- [9] H. Lynton and P.-Y. Siew, *Can. J. Chem.*, 51 (1973) 227.
- [10] S. Syoyama and K. Osaki, *Acta Crystallogr., Sect. B*, 28 (1972) 2626.
- [11] L. Pauling, *Z. Kristallogr.*, 72 (1930) 482.
- [12] W.C. Hamilton, *Acta Crystallogr.*, 15 (1962) 353.
- [13] R.E. Bachman, K.H. Whitmire, S. Mandal and P.K. Bharadwaj, *Acta Crystallogr., Sect. C*, 48 (1992) 1836.
- [14] G.J. Long and P.J. Clarke, *Inorg. Chem.*, 17 (1978) 1317.
- [15] D.J. Hamm, J. Bordner and A.F. Schreiner, *Inorg. Chim. Acta*, 7 (1973) 637.
- [16] B. Morosin, *Acta Crystallogr., Sect. B*, 31 (1975) 632.
- [17] W.L. Steffen and G.J. Palenik, *Acta Crystallogr., Sect. B*, 32 (1976) 298.
- [18] T.E. Gier and G.D. Stucky, *Nature (London)*, 349 (1991) 508.
- [19] *TEXSAN-TEXRAY, Structure Analysis Package*, Molecular Structure Corporation, The Woodlands, TX, 1985.
- [20] C.J. Gilmore, *J. Appl. Crystallogr.*, 17 (1984) 42.
- [21] P.T. Beurskins, *Tech. Rep. (1984/1)*, Crystallographic Laboratory, Toernooiveld, 6525 Ed Nijmegen, Netherlands.
- [22] W.A. Hamilton and J.A. Ibers, *Hydrogen Bonding in Solids*, W.A. Benjamin, Inc., New York, 1968.
- [23] K. Nakamoto, M. Margoshes and R.E. Rundle, *J. Am. Chem. Soc.*, 77 (1955) 6480.
- [24] A.B.P. Lever, *Inorganic Electronic Spectroscopy*, Elsevier, New York, 1984.
- [25] J.S. Merrimam and J.R. Perimareddi, *J. Phys. Chem.*, 79 (1975) 142.
- [26] C.K. Jorgensen, *Acta Chem. Scand.*, 9 (1955) 1362.